



# CHORUS

This is the accepted manuscript made available via CHORUS. The article has been published as:

## Crystal and magnetic structures of magnetic topological insulators $\text{MnBi}_{2}\text{Te}_{4}$ and $\text{MnBi}_{4}\text{Te}_{7}$

Lei Ding, Chaowei Hu, Feng Ye, Erxi Feng, Ni Ni, and Huibo Cao

Phys. Rev. B **101**, 020412 — Published 27 January 2020

DOI: [10.1103/PhysRevB.101.020412](https://doi.org/10.1103/PhysRevB.101.020412)

# Crystal and magnetic structures of magnetic topological insulators $\text{MnBi}_2\text{Te}_4$ and $\text{MnBi}_4\text{Te}_7$

Lei Ding,<sup>1,\*</sup> Chaowei Hu,<sup>2</sup> Feng Ye,<sup>1</sup> Erxi Feng,<sup>1</sup> Ni Ni,<sup>2</sup> and Huibo Cao<sup>1,†</sup>

<sup>1</sup>Neutron Scattering Division, Oak Ridge National Laboratory, Oak Ridge, TN 37831, USA

<sup>2</sup>Department of Physics and Astronomy and California NanoSystems Institute,  
University of California, Los Angeles, CA 90095, USA

(Dated: September 06, 2019)

Using single crystal neutron diffraction, we present a systematic investigation of the crystal structure and magnetism of van der Waals topological insulators  $\text{MnBi}_2\text{Te}_4$  and  $\text{MnBi}_4\text{Te}_7$ , where rich topological quantum states have been recently predicted and observed. Structural refinements reveal that considerable Bi atoms occupied on the Mn sites in both materials, distinct from the previously reported antisite disorder. We show unambiguously that  $\text{MnBi}_2\text{Te}_4$  orders antiferromagnetically below 24 K featured by a magnetic symmetry  $R\bar{1}3c$  while  $\text{MnBi}_4\text{Te}_7$  is antiferromagnetic below 13 K with a magnetic space group  $Pc\bar{3}c1$ . They both present antiferromagnetically coupled ferromagnetic layers with spins along the  $c$ -axis. We put forward a stacking rule for the crystal structure of an infinitely adaptive series  $\text{MnBi}_{2n}\text{Te}_{3n+1}$  ( $n \geq 1$ ) with the building unit of  $[\text{Bi}_2\text{Te}_3]$ . A comparison of magnetic properties between  $\text{MnBi}_2\text{Te}_4$  and  $\text{MnBi}_4\text{Te}_7$ , together with the recent density-functional theory calculations, enables us to draw that a two-dimensional magnetism limit might be realized in the derivatives. Our work may promote the theoretical studies of topological magnetic states in the series of  $\text{MnBi}_{2n}\text{Te}_{3n+1}$ .

*Introduction.* In condensed matter physics, van der Waals (vdW) magnetic heterostructures stacked layer-by-layer in a controlled sequence have attracted a great deal of interest as they have been found to show exotic physical properties and emergent phenomena [1–4]. Novel properties in these materials can be controlled by tuning the stacked atomic layers, paving the way for designing new quantum materials [1]. VdW magnetic topological insulators have been suggested as a promising material platform for the exploration of exotic topological quantum phenomena such as the quantum anomalous Hall effect (QAHE), Majorana fermions as well as topological magnetoelectric effect [4–7]. However, a homogenous heterostructure with intrinsic magnetism, an ideal platform for studying such topological quantum effects, is experimentally elusive [4].

Very recently,  $\text{MnBi}_2\text{Te}_4$  was proposed to be the first intrinsic antiferromagnetic (AFM) topological insulator [7–17]. It has been shown that below 24 K,  $\text{MnBi}_2\text{Te}_4$  orders into an A-type magnetic structure based on magnetic properties, density-functional theory calculations and powder neutron diffraction measurement [7, 13, 14, 18]. Since such a spin configuration breaks the product ( $S$ ) of the time-reversal symmetry and the primitive-lattice translational symmetry at the (001) surface, it is expected that a gapped surface Dirac cone can be observed by the angle-resolved photoemission spectroscopy (ARPES) made on the cleaved (001) surface [5, 12]. However, both gapped and gapless [8, 11, 13, 15] Dirac cones have been observed in ARPES measurements. This casts doubt on the magnetic configuration determined using the powder neutron diffraction data [7]. Furthermore, a new family of  $\text{MnBi}_{2n}\text{Te}_{3n+1}$  ( $n = 2, 3$ ) were later discovered [19, 20]. Among them,  $\text{MnBi}_4\text{Te}_7$  [19, 21, 22] and  $\text{MnBi}_6\text{Te}_{10}$  [19] have been suggested to be new magnetic topological insulators with weak interlayer magnetic coupling through a combined ARPES and first-principles calculations [21]. Although the A-type AFM was suggested for  $\text{MnBi}_4\text{Te}_7$  by its anisotropic magnetic properties, no neutron experiment has

been reported to prove it. Another riddle in both  $\text{MnBi}_2\text{Te}_4$  and  $\text{MnBi}_4\text{Te}_7$  is the saturated magnetic moment that is found to be about  $3 \mu_B$  in both cases [15, 17, 21, 22]. This is significantly smaller than  $5 \mu_B$  expected for the  $\text{Mn}^{2+}$  ion. To elucidate this reduction and unambiguously determine their magnetic structures, single crystal neutron diffraction experiment, which can map out the complete magnetic reflections with a better resolution, is urged.

Defects are of great importance in optimizing and understanding the surface states and magnetism in magnetic topological insulators [23, 24]. Antisite defects in  $\text{MnBi}_{2n}\text{Te}_{3n+1}$  have been found to be divergent. For example, by combining single-crystal x-ray diffraction and electron microscopy, Zeugner *et al.* have shown the presence of antisite disorder between Mn and Bi sites and Mn vacancies in the nominal  $\text{MnBi}_2\text{Te}_4$  which yield the composition  $\text{Mn}_{0.85(3)}\text{Bi}_{2.10(3)}\text{Te}_4$  [14] while Yan *et al.* later found the cationic disorder with only about 3% of the Bi sites occupied by Mn estimated by scanning tunnelling microscopy [18]. Similar defects have been reported in the nominal  $\text{MnBi}_4\text{Te}_7$  by x-ray diffraction and transmission electron microscopy [20, 22]. However, in light of the great difference of Mn and Bi in electronegativity, antisite defects are basically unfavourable. To rationally sort out the debate, it is natural to employ neutron diffraction technique as Mn and Bi atoms have opposite sign of the neutron scattering length.

Beyond the investigation of the magnetic structures, motivated by the above mentioned discoveries, our work is devoted to setting up the relationship between crystal structure and magnetic properties by examining the simple lattice-stacking rule starting from the prototype topological insulator  $\text{Bi}_2\text{Te}_3$  [25, 26]. Conventionally, its structure is described by the stacking of three “quintuple layer” building blocks [23, 27]. The bond coupling is rather strong between two atomic layers within one quintuple layer but much weaker, predominantly of the vdW type, between neighboring quintuple layers. Yet, “quintuple layer” stacking description does not re-

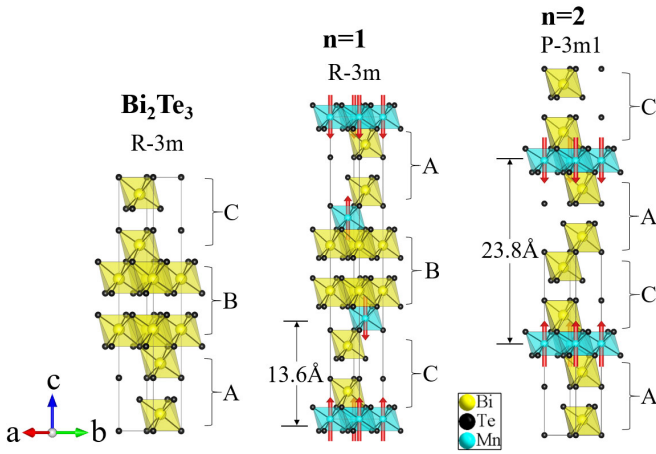


FIG. 1. Schematic drawings of the crystal structures of  $\text{Bi}_2\text{Te}_3$  and  $\text{MnBi}_{2n}\text{Te}_{3n+1}$  ( $n = 1, 2$ ). Note that for the latter cases, spin arrangements are denoted by red arrows.

fect the structural symmetry of  $\text{Bi}_2\text{Te}_3$  that may be important in understanding the topological properties in  $\text{MnBi}_{2n}\text{Te}_{3n+1}$ . The proposed stacking rule for building magnetic topological insulator Mn-Bi-Te series in this work practically captures the structural symmetry, reflects the precise layer stacking sequence, and reveals an infinitely adaptive series, stimulating theoretical calculations of exotic quantum states in the series of  $\text{MnBi}_{2n}\text{Te}_{3n+1}$ .

*Crystal structures of  $\text{MnBi}_2\text{Te}_4$  and  $\text{MnBi}_4\text{Te}_7$ .* We examined the crystal structure of both powder and single crystalline  $\text{MnBi}_2\text{Te}_4$  and  $\text{MnBi}_4\text{Te}_7$  samples using x-ray and neutron diffraction techniques [28]. For  $\text{MnBi}_2\text{Te}_4$ , the slice view of neutron diffraction data at 7 K is shown in Fig. 3(a) while the powder x-ray diffraction pattern is presented in [29]. For  $\text{MnBi}_4\text{Te}_7$ , Fig. 3(c) shows the contour map of neutron diffraction at 7 K, where the presence of sharp reflections indicates the high quality of the crystal. Single crystal neutron diffraction was also performed on the HB-3A DEMAND [30, 31] at room temperature on the same crystals [29]. We have refined both the single crystal neutron diffraction data from the DEMAND and x-ray powder diffraction data using the Fullprof software [32]. The refinement results as well as structural parameters are shown in Fig. 3 and Table S1-S4 [29], respectively. The refined lattice parameters are presented in Table I, which are in good agreement with the previous reports [19, 33]. Our refinement shows that about 18(1) % of Bi occupied at the Mn sites in the as-grown crystal  $\text{MnBi}_2\text{Te}_4$  whereas there is negligible Mn 1(1) % resided on the Bi sites [29]. This sort of non-stoichiometry effect becomes more robust in the  $\text{MnBi}_4\text{Te}_7$  crystal where there is 27.9(4) % of Bi on the Mn sites. Such results are substantially different from the intermixing between Mn and Bi sites and vacancies of Mn in  $\text{MnBi}_2\text{Te}_4$  and  $\text{MnBi}_4\text{Te}_7$  documented previously [13, 14, 18, 20, 22].

*Thermodynamic properties of  $\text{MnBi}_2\text{Te}_4$  and  $\text{MnBi}_4\text{Te}_7$ .* The ZFC temperature dependent magnetic susceptibilities of  $\text{MnBi}_2\text{Te}_4$  and  $\text{MnBi}_4\text{Te}_7$  measured with the field parallel to

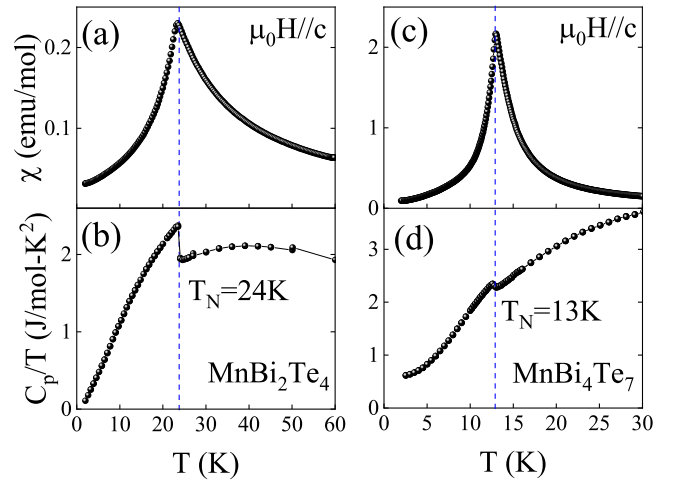


FIG. 2. Temperature dependence of the magnetic susceptibilities of  $\text{MnBi}_2\text{Te}_4$  (a) and  $\text{MnBi}_4\text{Te}_7$  (c) down to 2 K with magnetic field of 100 Oe under zero-field-cooling condition. Zero-field specific heat of  $\text{MnBi}_2\text{Te}_4$  (b) and  $\text{MnBi}_4\text{Te}_7$  (d) down to 2 K.

the  $c$ -axis are shown in Fig. 2. For the  $\text{MnBi}_2\text{Te}_4$  case, the susceptibility first increases with decreasing temperature and exhibits a sharp cusp at  $T_N = 24$  K, signaling the AFM ordering. In order to further characterize the magnetic phase transition, we measured the specific heat of  $\text{MnBi}_2\text{Te}_4$ . As shown in Fig. 2(b), the cusp at 24 K is indicative of the AFM transition, in good agreement with the magnetic susceptibility data. Thus  $\text{MnBi}_2\text{Te}_4$  only undergoes one AFM transition at 24 K. The magnetic susceptibility of  $\text{MnBi}_4\text{Te}_7$  shows a sharp peak at  $T_N = 13$  K (Fig. 2(c)), indicating an AFM transition. The nature of the transition can be crosschecked by the specific heat data of  $\text{MnBi}_4\text{Te}_7$ . As shown in Fig. 2(d), the specific heat shows a small anomaly at 13 K, consistent with the magnetic susceptibility results and the previous results.[21, 22] The Néel temperature of  $\text{MnBi}_4\text{Te}_7$  is about two times smaller than that of  $\text{MnBi}_2\text{Te}_4$ .

*A-type magnetic structure of  $\text{MnBi}_2\text{Te}_4$  and  $\text{MnBi}_4\text{Te}_7$ .* The magnetic structure of  $\text{MnBi}_2\text{Te}_4$  has been previously investigated using powder neutron diffraction [18]. They found that the AFM structure has the magnetic symmetry  $P_c-3c1$  (BNS symbol) propagated by a vector  $\mathbf{k}=(0, 0, 1/2)$ , which is a lower magnetic symmetry than that determined from our neutron data. As shown in Fig. 3(a), our neutron diffraction experiment reveals that a set of magnetic reflections, which appears at 7 K, can be indexed by a vector  $\mathbf{k}=(0, 0, 3/2)$ . As a matter of fact, the magnetic reflections shown in Ref. [18] should be reasonably indexed by this vector, implying that the proposed magnetic space group should be reconsidered here. To solve the magnetic structure of  $\text{MnBi}_2\text{Te}_4$ , we have carried out the magnetic symmetry analysis by considering the  $\mathbf{k}$  vector and the parent space group  $R-3m1'$  with help of the ISODISTORT software [34] and Bilbao Crystallography Server [35]. There are two active magnetic irreducible representations,  $mT2+$  and  $mT3+$ . After testing these candidates, we found the irrep  $mT2+$ , corresponding to the magnetic space group  $R_I-3c$ , is the only solution while the latter irrep  $mT3+$  conveying three

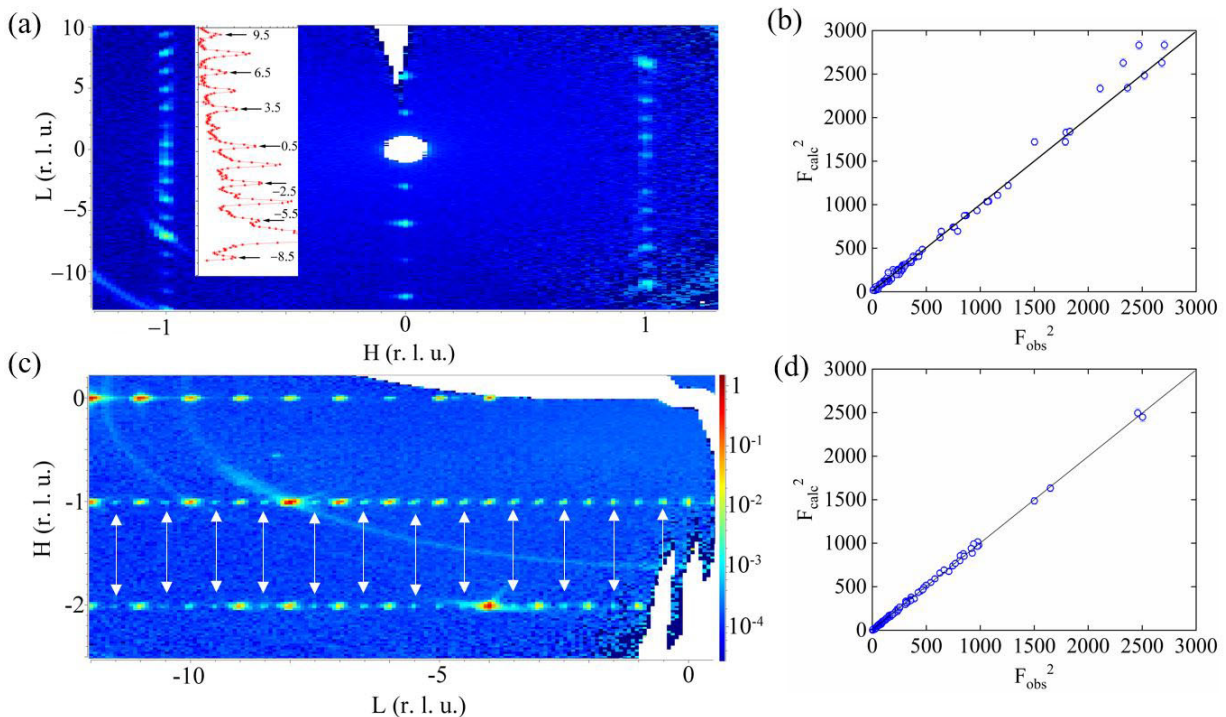


FIG. 3. (a) Contour map of neutron intensity of  $\text{MnBi}_2\text{Te}_4$  in the  $(H\ 0\ L)$  reciprocal plane at 7 K measured on the CORELLI. (b) The results for the nuclear and magnetic structure refinements of  $\text{MnBi}_2\text{Te}_4$  at 4.5 K with neutron data from the DEMAND. (c) Contour map of neutron intensity of  $\text{MnBi}_4\text{Te}_7$  in the  $(H\ 0\ L)$  reciprocal plane at 7 K measured on the CORELLI. Arrows mark the magnetic reflections. (d) The results for the nuclear and magnetic structure refinements of  $\text{MnBi}_4\text{Te}_7$  at 4.5 K with neutron data from the DEMAND

different magnetic structures is incompatible with our neutron data [29]. Magnetic neutron diffraction data measured at 4.5 K on the DEMAND were then refined using the magnetic symmetry  $R\bar{1}-3c$  and the results of the refinement is shown in Fig. 3(b). It turns out that spins line up ferromagnetically in the  $ab$  plane below 24 K whereas between layers, magnetic moments are antiparallel. The refined magnetic moment of  $\text{Mn}^{2+}$  at 4.5 K is  $4.7(1)\mu_B$ , in good accordance with the expected totally ordered moment  $5\mu_B$  for  $\text{Mn}^{2+}$  ion.

Single crystal neutron diffraction data of  $\text{MnBi}_4\text{Te}_7$  show clearly the appearance of magnetic reflections at the  $(H\ 0\ L+0.5)$  positions ( $H, L$  denote the Miller index) upon cooling below 13 K, confirming the formation of a long-range AFM order. As shown in Fig. 3(c) all magnetic reflections can be indexed by the propagation vector  $\mathbf{k}=(0, 0, 1/2)$ . Starting with the parent space-group  $P-3m1'$  and the propagation vector  $\mathbf{k}$  in A point in the Brillouin zone, through ISODISTORT, two active magnetic irreducible representations,  $\text{mA}1-$  and  $\text{mA}3-$  were obtained. We found that magnetic space group  $P_c-3c1$  (BNS symbol, basis= $(1,0,0),(0,1,0),(0,0,2)$ , origin= $(0, 0, 1/2)$ ), generated from the single active  $\text{mA}1-$ , can be adopted to describe the magnetic structure. Magnetic structure model was refined on the neutron data collected at 4.5 K on the DEMAND. The refined magnetic structure is characteristic of an AFM arrangement between the adjacent FM layers, as shown in Fig 1. The refined total magnetic moment at 4.5 K is  $4.01(9)\mu_B$  along the  $c$ -axis, relatively smaller than the value of  $5\mu_B$  expected for  $S = 5/2$  of  $\text{Mn}^{2+}$ . Here, the

small discrepancy is likely because it is not fully ordered yet at 4.5 K, indicated by the ordering parameter shown below. It appears that  $\text{MnBi}_4\text{Te}_7$  bears a similar spin arrangement between layers (different magnetic symmetry) to  $\text{MnBi}_2\text{Te}_4$  but magnetically orders at a much lower temperature due to the increased distance between magnetic Mn-layers.

The seemingly reduced saturated magnetic moment in both  $\text{MnBi}_2\text{Te}_4$  and  $\text{MnBi}_4\text{Te}_7$  can be reasonably understood by our neutron diffraction results. The deficiency of Mn on the Mn sites in both cases naturally explains the small saturated magnetic moments detected by the bulk magnetization. As determined by the neutron diffraction, the ordered magnetic moment of Mn is reasonably close to the theoretical value.

Having known the magnetic structures of the vdW magnets with  $n = 1, 2$ , we now examine the temperature dependence of the strongest magnetic reflections for each case. The temperature-dependent intensity of the magnetic reflections ( $-1\ 0\ 0.5$ ) and  $(0\ 1\ 1.5)$  for  $\text{MnBi}_2\text{Te}_4$  and  $\text{MnBi}_4\text{Te}_7$ , respectively are shown in Fig. 4. They may follow an empirical power-law behavior [36, 37],

$$I = A \left( \frac{T_M - T}{T_M} \right)^{2\beta} + B \quad (1)$$

where  $T_M$  is the critical temperature for magnetic phase transitions,  $A$  is a proportionality constant,  $\beta$  is the order parameter critical exponent and  $B$  is the background. Fits to the power law were performed for two temperature regions for the two cases. The best fit in the temperature ranges of 21-30 K and 9-20 K yields the Neél temperatures  $T_N=24.8(1)$  K

TABLE I. Derivatives of the vdW  $\text{MnBi}_{2n}\text{Te}_{3n+1}$  topological insulators. Lattice parameters (i: experiment, ii: prediction) are shown at room temperature. The lattice parameters for each sequence of the stacking units are based on  $\text{Bi}_2\text{Te}_3$ :  $a=b=4.3896(2)$  Å,  $c=30.5019(10)$  Å [27]. When  $n=2+3m$  ( $m = 0, 1, 2, \dots$ ), the lattice of derivatives is primitive. The predicted magnetic space groups (MSG) are made based on a symmetry analysis using the  $\mathbf{k}$  vectors of  $(0, 0, 3/2)$  for the rhombohedral lattice,  $(0, 0, 1/2)$  for the hexagonal lattice,  $(0, 0, 0)$  for the cases with ferromagnetic (FM) order.

n	Sequence	SG	Lattice parameter		Magnetic properties and MSG
1	<i>M-C-M-B-M-A-M</i>	<i>R-3m</i>	4.3336(2) Å	40.926(3) Å [i, this work]	AFM, <i>R<sub>1</sub>-3c</i> [i, this work]
2	<i>A-M-C</i>	<i>P-3m1</i>	4.3453(5) Å	23.705(3) Å [i, this work]	AFM, <i>Pc-3c1</i> [i, this work]
3	<i>M-C-A-B-M-A-B-C-M-B-C-A-M</i>	<i>R-3m</i>	4.3745(3) Å	101.985(8) Å [i][19]	AFM, <i>R<sub>1</sub>-3c</i> [ii]
4	<i>M-C-A-B-C-M-B-C-A-B-M-A-B-C-A-M</i>	<i>R-3m</i>	4.37485(3) Å	132.416(2) Å [ii]	FM, <i>R-3m</i> [ii]
5	<i>M-C-A-B-C-A-M</i>	<i>P-3m1</i>		132.45 Å [ii]	
6	<i>M-C-A-B-C-A-B-M-A-B-C-A-B-C-M-B-C-A-B-C-A-M</i>	<i>R-3m</i>		54.32 Å [ii]	FM <i>P-3m1</i> [ii]
				193.47 Å [ii]	FM, <i>R-3m</i> [ii]

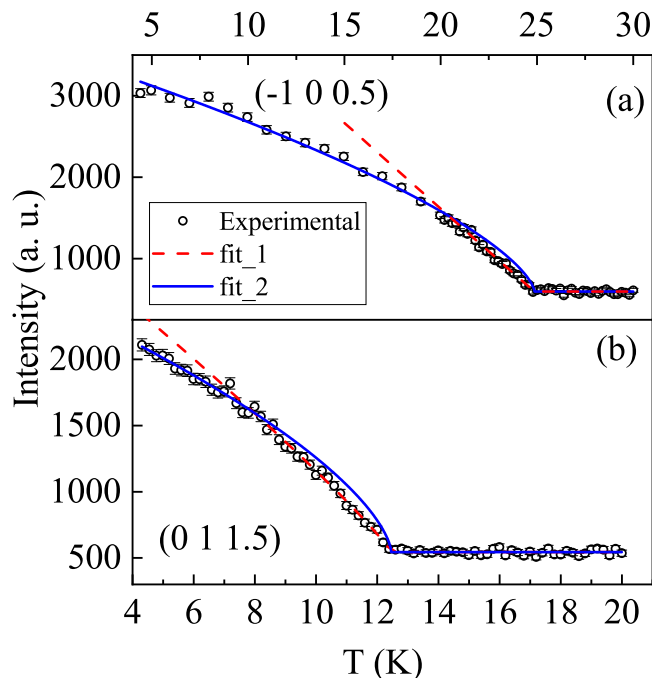


FIG. 4. Magnetic order parameter upon warming at the magnetic reflections  $(-1\ 0\ 0.5)$  and  $(0\ 1\ 1.5)$  for  $\text{MnBi}_2\text{Te}_4$  (a) and  $\text{MnBi}_4\text{Te}_7$  (b) measured at DEMAND, respectively. Dashed and solid lines represent the results of a power-law fits in different temperature regions.

and 12.5(1)K, the critical exponents  $\beta=0.50(5)$  and 0.45(3) for  $\text{MnBi}_2\text{Te}_4$  and  $\text{MnBi}_4\text{Te}_7$ , respectively. Both critical exponents determined in the two temperature regions that are within the critical regions are in accordance with that of the Ginzburg-Landau theory. In the temperature range of 4.5-21 K, the best fit for  $\text{MnBi}_2\text{Te}_4$  yields the critical exponent  $\beta=0.32(1)$ , a value relatively smaller than the results in Ref.[18]. This  $\beta$  value is in fact very close to the value, 0.325, expected for a universality class of the three-dimensional Ising model[36]. In the lower temperature range  $4.5\text{ K} < T < 9\text{ K}$ , the critical exponent  $\beta=0.32(2)$  of  $\text{MnBi}_4\text{Te}_7$  is very close

to that of  $\text{MnBi}_2\text{Te}_4$ . This seems to be contradictory to the less three-dimensional magnetism in  $\text{MnBi}_4\text{Te}_7$  caused by the much larger interlayer Mn-Mn distance. The reason may lie in the fact that the fitting for the  $\text{MnBi}_4\text{Te}_7$  case was done in a temperature range that is relatively close to the critical region which often comes with a crossover from three-dimensional to two-dimensional behavior upon cooling [37, 38].

*Stacking rule and crystal structures of vdW  $\text{MnBi}_{2n}\text{Te}_{3n+1}$ .* Based on the crystal structure of  $\text{MnBi}_2\text{Te}_4$ ,  $\text{MnBi}_4\text{Te}_7$ , as shown in Fig. 1, we can put forward a stacking rule of the crystal structure of this family that is based on the rhombohedral lattice of  $\text{Bi}_2\text{Te}_3$ . The aforementioned structural description of the  $\text{Bi}_2\text{Te}_3$  is based on the stacking of three “quintuple layer” building blocks. This description has been used to predict the infinitely adaptive series of thermoelectric materials [23, 39]. However, it seemingly does not capture the essential structural symmetry but rather simply depicts the stacking lattice. As shown in Fig. 1, the crystal structure of  $\text{Bi}_2\text{Te}_3$  is designated as A-B-C stacking sequence with A, B and C representing distinct  $[\text{Bi}_2\text{Te}_3]$  units. Imposed by the inversion and rhombohedral centering translation, the A unit can be progressed into B, and subsequently C configuration. Simply, we introduce magnetic atoms by inserting M (M denotes  $\text{MTe}_6$  octahedra layer) layers into this A-B-C stacking sequence, giving rise to an infinitely adaptive series  $\text{MnBi}_{2n}\text{Te}_{3n+1}$ . Accordingly, we can immediately name the sequence *M-C-M-B-M-A-M* with  $n = 1$  which preserves the crystal symmetry *R-3m*. This yields the compound  $\text{MnBi}_2\text{Te}_4$ , as illustrated in Fig. 1. With  $n = 2$ , where one more  $[\text{Bi}_2\text{Te}_3]$  unit is added, we get the stacking sequence *A-M-C* with the space group *P-3m1*. It corresponds to the compound  $\text{MnBi}_4\text{Te}_7$ , indicating a great compatibility between these structural units. It occurs that the B-type unit occurring in  $\text{MnBi}_2\text{Te}_4$  disappears in  $\text{MnBi}_4\text{Te}_7$ . Consequently, this leads to a general stacking rule for a vast number of vdW magnets in this family: the magnetic Mn-layer can replace one of A, B or C-type unit but still leaves the -A-B-C- stacking sequence unchanged. Indeed, with the increment of the value of  $n$  ( $n \geq 1$ ), the sequence of the building units, crystal symmetry and lattice parameters of

the corresponding vdW magnet can be generated and listed in Table I. Following this stacking rule, one can make an infinitely adaptive series as those listed in Table I (here we only list up to  $n = 6$ ).

*Magnetism of  $MnBi_{2n}Te_{3n+1}$  derivatives.* Recently, theoretical calculations on  $MnBi_2Te_4$  [12] have shown that in the ( $ab$ ) plane the FM interaction between the first nearest neighbors  $J_1=1.693$  meV strongly dominates over all others. By considering all the exchange interactions in the layer and magnetic anisotropy energy, they suggest the FM ordering temperature of  $T_c=12(1)K$  in a single free-standing  $MnBi_2Te_4$  septuple layer [12]. Interestingly,  $MnBi_4Te_7$  orders antiferromagnetically at 13 K, very close to the aforementioned 12(1) K. This indicates that in  $MnBi_4Te_7$  intralayer exchange interaction is robust whereas the interlayer one is minimal. Indeed, recent calculations on  $MnBi_4Te_7$  yielded that  $J_1$  and  $J_\perp$  (a summed exchange coupling between the adjacent layers) [21, 22] are 1.704 meV and -0.150 meV, respectively. With the increase of non-magnetic building units, FM could be realized by quenching all interlayer exchange interactions. Therefore, for  $MnBi_{2n}Te_{3n+1}$  with  $n>2$ , if we assume their magnetic ground state to be either A-type AFM or FM with all magnetic moments being aligned along the  $c$ -axis, the magnetic space group for each compound is predicted and presented in Table I. Experiments to characterize other derivatives and to ascertain the predicted magnetic space groups are called.

*Conclusion.* In summary, we have investigated systematically the crystal structure and magnetism of vdW topological insulators  $MnBi_2Te_4$  and  $MnBi_4Te_7$ . Considerable Mn deficiency has been found on the Mn sites for both cases. Our results have shown that the ordered magnetic moments of  $MnBi_2Te_4$  and  $MnBi_4Te_7$  are reasonably close to the expected  $5 \mu_B$  for  $Mn^{2+}$  ion. We have revealed a simple lattice-stacking rule that can lead to an infinitely adaptive series of  $MnBi_{2n}Te_{3n+1}$ . Although different magnetic symmetry exists in  $MnBi_2Te_4$  and  $MnBi_4Te_7$  with the former being  $R\bar{1}-3c$  and the latter being  $P_c-3c1$ , our single crystal neutron diffraction measurements have unambiguously established that in the ordered state, both compounds show the A-type AFM structure with all spins parallel in the  $ab$  plane but antiparallel along the  $c$  axis which is critical for the observation of quantized anomalous Hall effect when they are exfoliated down to a few layers.

*Acknowledgements.* We thank C. D. Batista for useful discussions. The research at Oak Ridge National Laboratory (ORNL) was supported by the U.S. Department of Energy (DOE), Office of Science, Office of Basic Energy Sciences, Early Career Research Program Award KC0402010, under Contract DE-AC05-00OR22725 and the U.S. DOE, Office of Science User Facility operated by the ORNL. Work at UCLA was supported by the U.S. Department of Energy (DOE), Office of Science, Office of Basic Energy Sciences under Award Number DE-SC0011978. The US Government retains, and the publisher, by accepting the article for publication, acknowledges that the US Government retains a nonexclusive, paid-up, irrevocable, worldwide license to publish or reproduce the published form of this manuscript, or allow others

to do so, for US Government purposes. The Department of Energy will provide public access to these results of federally sponsored research in accordance with the DOE Public Access Plan [40].

---

\* [dingl@ornl.gov](mailto:dingl@ornl.gov)

† [caoh@ornl.gov](mailto:caoh@ornl.gov)

- [1] A. K. Geim and K. S. Novoselov, “The rise of graphene,” *Nature Mater.* **6**, 183 (2007).
- [2] C. Gong *et al.*, “Discovery of intrinsic ferromagnetism in two-dimensional van der Waals crystals,” *Nature* **546**, 265–269 (2017).
- [3] B. Huang *et al.*, “Layer-dependent ferromagnetism in a van der waals crystal down to the monolayer limit,” *Nature* **546**, 270–273 (2017).
- [4] Y. Tokura, K. Yasuda, and A. Tsukazaki, “Magnetic topological insulators,” *Nature Reviews Physics* **1**, 126–143 (2019).
- [5] R. S. K. Mong, A. M. Essin, and J. E. Moore, “Antiferromagnetic topological insulators,” *Phys. Rev. B* **81**, 245209 (2010).
- [6] Xiao-Gang Wen, “Choreographed entanglement dances: Topological states of quantum matter,” *Science* **363**, 6429 (2019).
- [7] J. H. Li, Y. Li, S. Q. Du, Z. Wang, B.-L. Gu, S.-C. Zhang, K. He, W. H. Duan, and Y. Xu, “Intrinsic magnetic topological insulators in van der waals layered  $MnBi_2Te_4$ -family materials,” *Sci. Adv.* **5**, eaaw5685 (2019).
- [8] Y. J. Hao *et al.*, “Gapless surface dirac cone in antiferromagnetomagnetic topological insulator  $MnBi_2Te_4$ ,” arXiv:1907.03722.
- [9] D. Q. Zhang, M. J. Shi, T. S. Zhu, D. Y. Xing, H. J. Zhang, and J. Wang, “Topological axion states in the magnetic insulator  $MnBi_2Te_4$  with the quantized magnetoelectric effect,” *Phys. Rev. Lett.* **122**, 206401 (2019).
- [10] T. Hirahara *et al.*, “Large-gap magnetic topological heterostructure formed by subsurface incorporation of a ferromagnetic layer,” *Nano Lett.* **17**, 3493–3500 (2017).
- [11] Y. Gong *et al.*, “Experimental realization of an intrinsic magnetic topological insulator,” *Chin. Phys. Lett.* **36**, 076801 (2019).
- [12] M. M. Otrokov *et al.*, “Unique thickness-dependent properties of the van der waals interlayer antiferromagnet  $MnBi_2Te_4$  films,” *Phys. Rev. Lett.* **122**, 107202 (2019).
- [13] M. M. Otrokov *et al.*, “Prediction and observation of the first antiferromagnetic topological insulator,” arXiv:1809.07389.
- [14] A. Zeugner *et al.*, “Chemical aspects of the candidate antiferromagnetic topological insulator  $MnBi_2Te_4$ ,” *Chem. Mater.* **31**, 2795–2806 (2019).
- [15] B. Chen *et al.*, “Searching the  $Mn(Sb,Bi)_2Te_4$  family of materials for the ideal intrinsic magnetic topological insulator,” arXiv:1903.09934.
- [16] Y. J. Deng, Y. J. Yu, M. Z. Shi, J. Wang, X. H. Chen, and Y. B. Zhang, “Magnetic-field-induced quantized anomalous hall effect in intrinsic magnetic topological insulator  $MnBi_2Te_4$ ,” arXiv:1904.11468.
- [17] S. H. Lee *et al.*, “Spin scattering and noncollinear spin structure-induced intrinsic anomalous hall effect in antiferromagnetic topological insulator  $MnBi_2Te_4$ ,” *Phys. Rev. Research* **1**, 012011 (2019).
- [18] J.-Q. Yan, Q. Zhang, T. Heitmann, Zengle Huang, K. Y. Chen, J.-G. Cheng, Weida Wu, D. Vaknin, B. C. Sales, and R. J. McQueeney, “Crystal growth and magnetic structure of  $MnBi_2Te_4$ ,” *Phys. Rev. Mater.* **3**, 064202 (2019).

- [19] Z. S. Aliev *et al.*, “Novel ternary layered manganese bismuth tellurides of the MnTe-Bi<sub>2</sub>Te<sub>3</sub> system: Synthesis and crystal structure,” *J. Alloys Compd.* **789**, 443–450 (2019).
- [20] D. Souchay, M. Nentwig, D. Gunther, S. Keilholz, J. de Boor, A. Zeugner, A. Isaeva, M. Ruck, A. U. B. Wolter, B. Buchner, and O. Oeckler, “Layered manganese bismuth tellurides with GeBi<sub>4</sub>Te<sub>7</sub>- and GeBi<sub>6</sub>Te<sub>10</sub>-type structures: towards multifunctional materials,” *J. Mater. Chem. C* **7**, 9939 (2019).
- [21] C.-W. Hu *et al.*, “A van der waals antiferromagnetic topological insulator with weak interlayer magnetic coupling,” arXiv:1905.02154.
- [22] R. C. Vidal *et al.*, “Topological electronic structure and intrinsic magnetization in MnBi<sub>4</sub>Te<sub>7</sub>: a Bi<sub>2</sub>Te<sub>3</sub>-derivative with a periodic Mn sublattice,” arXiv:1906.08394.
- [23] R. J. Cava, Huiwen Ji, M. K. Fuccillo, Q. D. Gibson, and Y. S. Hor, “Crystal structure and chemistry of topological insulators,” *J. Mater. Chem. C* **1**, 3176–3189 (2013).
- [24] Y. S. Hor, P. Roushan, H. Beidenkopf, J. Seo, D. Qu, J. G. Checkelsky, L. A. Wray, D. Hsieh, Y. Xia, S.-Y. Xu, D. Qian, M. Z. Hasan, N. P. Ong, A. Yazdani, and R. J. Cava, “Development of ferromagnetism in the doped topological insulator Bi<sub>2-x</sub>Mn<sub>x</sub>Te<sub>3</sub>,” *Phys. Rev. B* **81**, 195203 (2010).
- [25] H. J. Zhang, C. X. Liu, X. L. Qi, X. Dai, Z. Fang, and S. C. Zhang, “Topological insulators in Bi<sub>2</sub>Se<sub>3</sub>, Bi<sub>2</sub>Te<sub>3</sub> and Sb<sub>2</sub>Te<sub>3</sub> with a single dirac cone on the surface,” *Nature Phys.* **5**, 438–442 (2009).
- [26] Y. L. Chen *et al.*, “Experimental realization of a three-dimensional topological insulator, Bi<sub>2</sub>Te<sub>3</sub>,” *Science* **325**, 178–182 (2009).
- [27] V.V. Atuchin, T.A. Gavrilova, K.A. Kokh, N.V. Kuratieva, N.V. Pervukhina, and N.V. Surovtsev, “Structural and vibrational properties of pvt grown Bi<sub>2</sub>Te<sub>3</sub> microcrystals,” *Solid State Commun.* **152**, 1119–1122 (2012).
- [28] F. Ye, Y. Liu, R. Whitfield, R. Osborn, and S. Rosenkranz, “Implementation of cross correlation for energy discrimination on the time-of-flight spectrometer CORELLI,” *J. Appl. Crystallogr.* **51**, 315–322 (2018).
- [29] See Supplemental Material for experimental methods and the description of the crystal structure refinement and magnetic structure determination.
- [30] B. C. Chakoumakos, H. B. Cao, F. Ye, A. D. Stolica, M. Popovici, M. Sundaram, W. Zhou, J. S. Hicks, G. W. Lynn, and R. A. Riedel, “Symmetry-based computational tools for magnetic crystallography,” *J. Appl. Crystallogr.* **44**, 655 (2011).
- [31] H. B. Cao, B. C. Chakoumakos, K. M. Andrews, Y. Wu, R. A. Riedel, J. Hodges, W. D. Zhou, R. Gregory, B. Haberi, J. Molaison, and G. W. Lynn, “Demand, a dimensional extreme magnetic neutron diffractometer at the high flux isotope reactor,” *Crystals* **9**, 5 (2019).
- [32] J. Rodríguez-Carvajal, “Recent advances in magnetic structure determination by neutron powder diffraction,” *Phys. B Condens. Matter* **192**, 55 (1993).
- [33] D. S. Lee, T.-H. Kim, C.-H. Park, C.-Y. Chung, Y. S. Lim, W.-S. Seo, and H.-H. Park, “Crystal structure, properties and nanostructuring of a new layered chalcogenide semiconductor, Bi<sub>2</sub>MnTe<sub>4</sub>,” *CrystEngComm* **15**, 5532–5538 (2013).
- [34] B. J. Campbell, H. T. Stokes, Tanner D. E., and D. M. Hatch, “Isodisplace: An internet tool for exploring structural distortions,” *J. Appl. Crystallogr.* **39**, 607 (2006).
- [35] J. M. Perez-Mato, S. V. Gallego, E. S. Tasci, L. Elcoro, G. de la Flor, and M. I. Aroyo, “Symmetry-based computational tools for magnetic crystallography,” *Ann. Rev. Mater. Res.* **45**, 217 (2015).
- [36] S. G. Brush, “History of the lenz-ising model,” *Rev. Mod. Phys.* **39**, 883–893 (1967).
- [37] R. J. Birgeneau, H. J. Guggenheim, and G. Shirane, “Neutron scattering investigation of phase transitions and magnetic correlations in the two-dimensional antiferromagnets K<sub>2</sub>NiF<sub>4</sub>, Rb<sub>2</sub>MnF<sub>4</sub>, Rb<sub>2</sub>FeF<sub>4</sub>,” *Phys. Rev. B* **1**, 2211–2230 (1970).
- [38] A. R. Wildes, H. M. Rønnow, B. Roessli, M. J. Harris, and K. W. Godfrey, “Static and dynamic critical properties of the quasi-two-dimensional antiferromagnet MnPS<sub>3</sub>,” *Phys. Rev. B* **74**, 094422 (2006).
- [39] J. W. G. Bos, H. W. Zandbergen, M.-H. Lee, N. P. Ong, and R. J. Cava, “Structures and thermoelectric properties of the infinitely adaptive series (Bi<sub>2</sub>)<sub>m</sub>(Bi<sub>2</sub>Te<sub>3</sub>)<sub>n</sub>,” *Phys. Rev. B* **75**, 195203 (2007).
- [40] <https://www.energy.gov/downloads/doe-public-access-plan>.